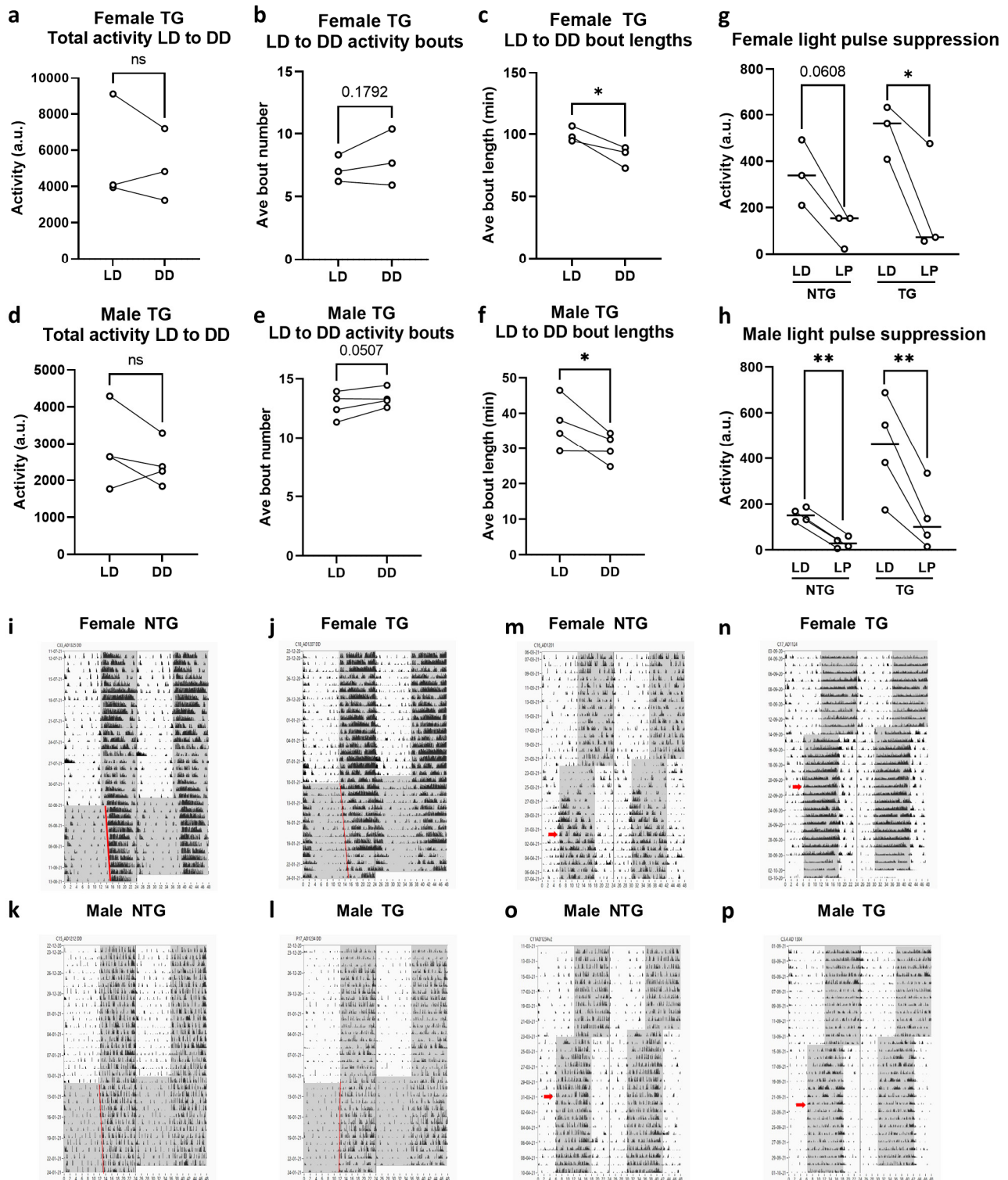
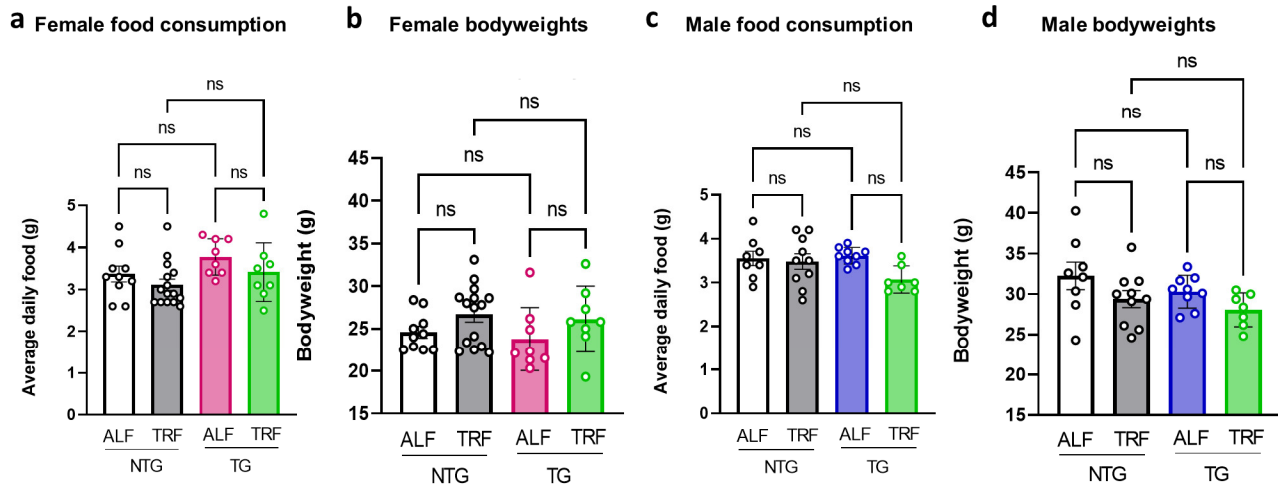


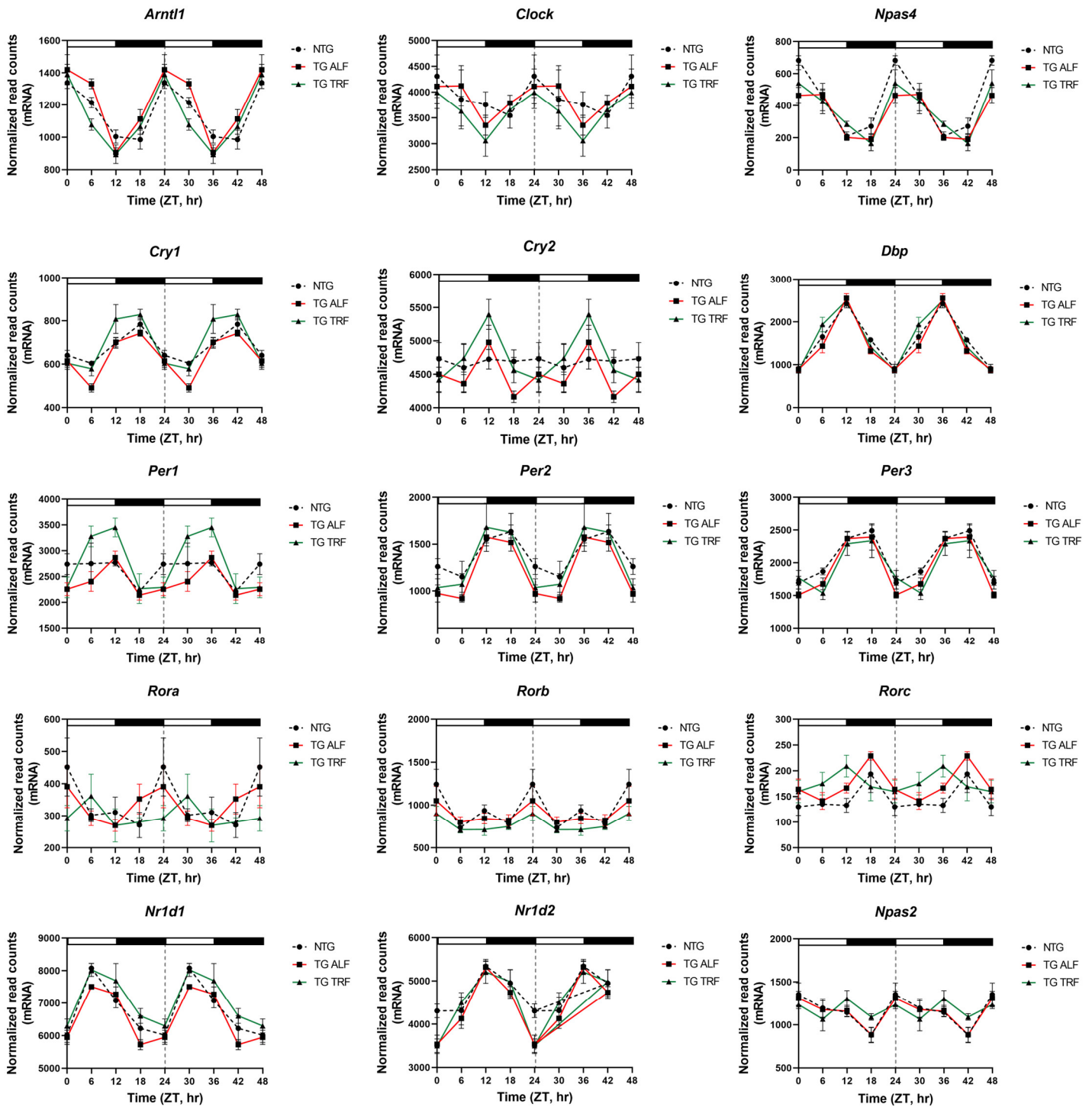
**Supplemental data figure 1. APP23 TG mice show sleep and activity alterations, related to figure 1.** Immobility-defined sleep and cage locomotor activity were recorded in single-housed mice using surveillance cameras and IR sensors, respectively. **a-b.** Sleep data were analyzed over two 24 h sleep-wake cycles. Sleep waveforms are represented as average sleep per hour. **c-d.** Activity recordings reported in 6 h bins averaged from 7-10 days of activity. Top bar in waveforms represents the light-dark cycle. Statistical significance represented one-way ANOVA followed by multiple comparisons using the Holm-Šidák method (a-b), one-way ANOVA followed by Šidák's multiple comparisons test (c-d) \* $p \leq 0.05$ ; \*\* $p \leq 0.01$ ; \*\*\*\*  $p \leq 0.0001$ .



**Supplemental data figure 2. APP23 TG mice show circadian alterations, related to figure 1.** Light/dark (LD), constant darkness (DD), 6 h phase advance, and light pulse conditions were recorded using IR sensors from mice single-housed in circadian cabinets. **a-f.** Total activity, average number of activity bouts and average bout lengths in DD compared to the same TG mice in LD. **g-h.** Activity suppression in response to a 1 h long light pulse (LP; negative light masking) in the dark phase compared to a prior non-pulsed hour (LD) at the same time. **i-l.** Representative actograms illustrating activity rhythms under LD and DD conditions with grey areas representing lights out and red bars denoting activity onset in DD. **m-p.** Representative actograms illustrating activity rhythms under LD and in response to a 6 h phase advance signified by the shifted grey (active phase) region. Red arrows indicate the point of entrainment to the new LD cycle. Actograms are double plotted (48 h/line) with consecutive days shown top to bottom and X-axis in ZT h. Bar graphs represent individual data plots with standard error of the mean. Statistical significance represents the comparison between LD and DD or LP as per paired Student's *t*-test \* $p \leq 0.05$ ; \*\* $p \leq 0.01$ .

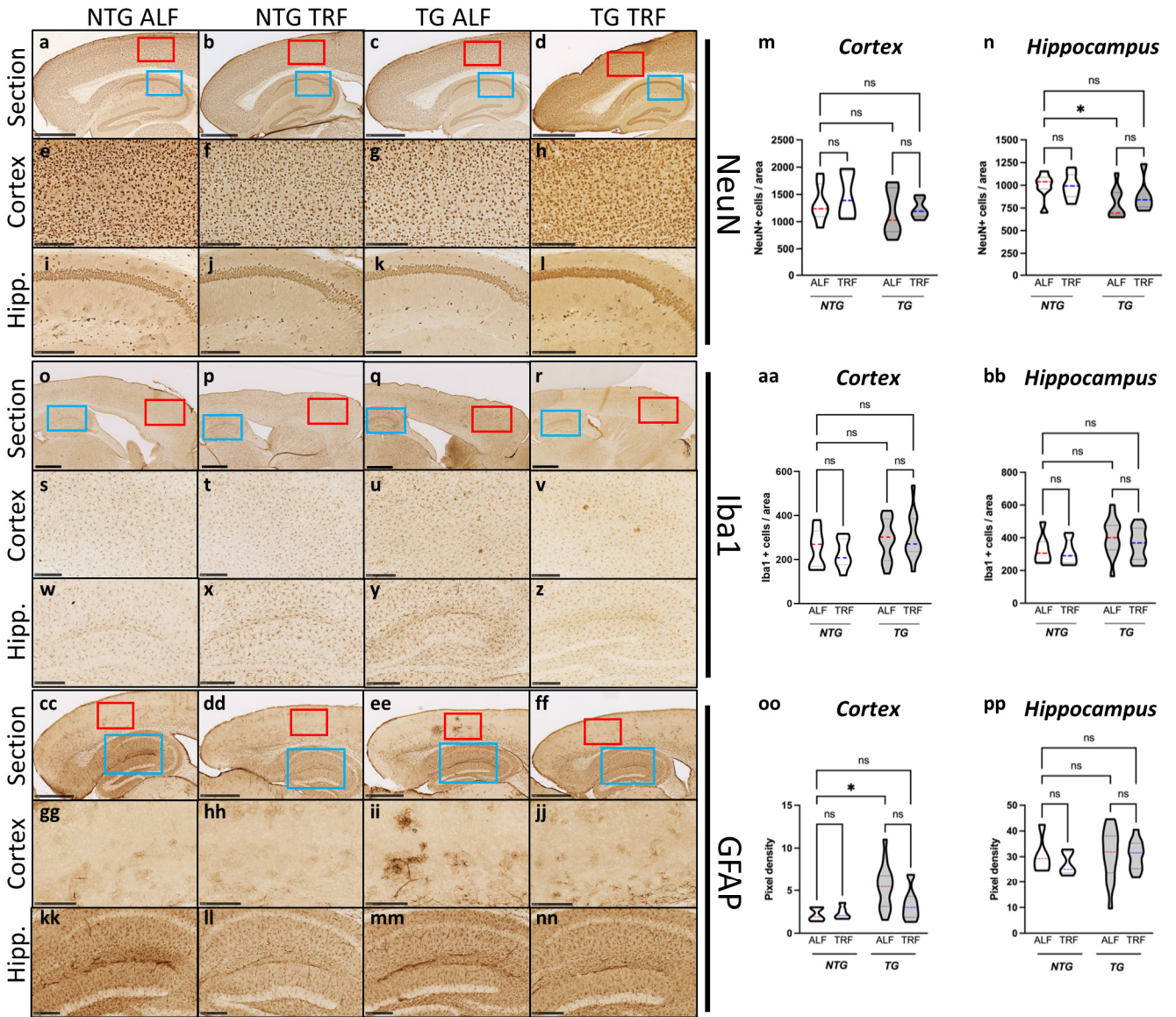


**Supplemental data figure 3. Food weights and body weights under time-restricted feeding, related to figure 2. a-d.** The TRF regimen did not alter caloric intake calculated as total food consumption or body weights in comparison to ALF. Statistical significance represents one-way ANOVA with Tukey's multiple comparisons test.

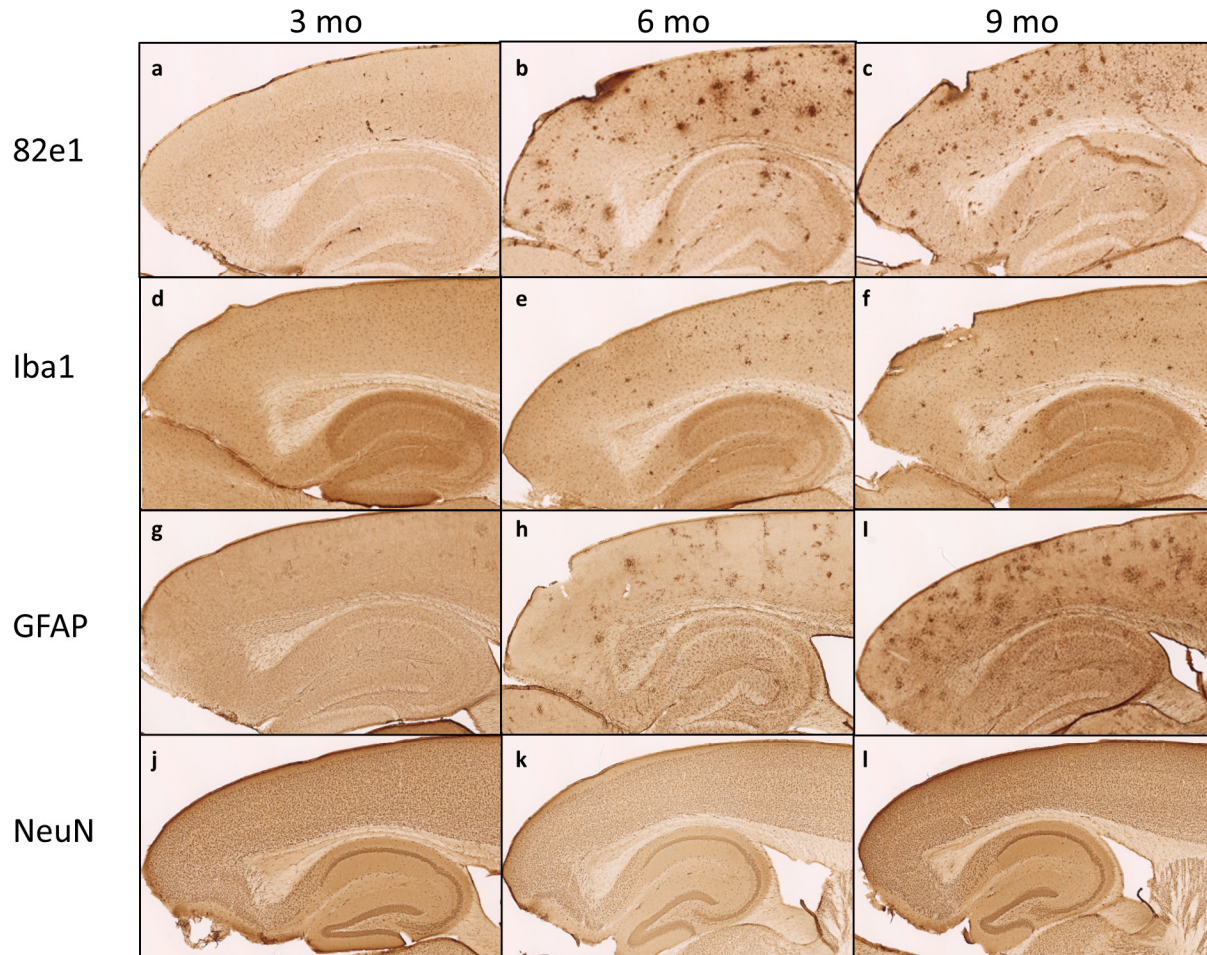


**Supplemental data figure 4. Effects of TRF on the expression of core clock genes in the hippocampus, related to figures 1 and 3.** Normalized read counts from RNA-Seq analysis in NTG, TG ALF and TG TRF mice. Grey dashed line indicates double-plotting of waveforms and bars above represent the light-dark cycle.





**Supplemental data figure 5. Neuropathology in APP23 TG under time-restricted feeding, related to figure 5.** Immunoassayed slides were scanned in a Nanozoomer and images were processed in ImageJ for quantification of immunopositive particles. **a-l.** Immunostaining of NeuN+ nuclei. **m-n.** Quantification of NeuN+ nuclei. **o-z.** Immunostaining of Iba1+ microglia. **aa-bb.** Quantification of Iba1+ microglia. **cc-nn.** Immunostaining of GFAP+ astrocytes. **oo-pp.** Quantification of GFAP+ astrocytes. Red boxes represent the enlarged cortex region. Blue boxes represent the enlarged hippocampal sections. Scale bars represent 1 mm for section and 250  $\mu$ m for enlarged cortex and hippocampal regions. Statistical significance in violin plots represents one-way ANOVA with Tukey's multiple comparisons test \*  $p < 0.05$ .



**Supplemental data figure 6. Neuropathology in APP-KI at 3-, 6- and 9-months, related to figure 6.** Images obtained by scanning slides in a Nanozoomer. **a-c.** Immunostaining of 82E1+ plaques. **d-f.** Immunostaining of Iba1+ microglia. **g-i.** Immunostaining of GFAP+ astrocytes. **j-l.** Immunostaining of NeuN+ neurons.